LINEAR OPTICS DESIGN FOR PS2

Y. Papaphilippou, W. Bartmann, M. Benedikt, C. Carli,
B. Goddard, S. Hancock, J. M. Jowett, A. Koschik,
CERN, Geneva, Switzerland

Abstract

The design considerations and key parameters for the replacement of the CERN Proton Synchrotron (PS) with a new ring (PS2), as part of the upgrade of the LHC injector complex are summarized. Classical linear optics solutions including standard FODO, doublet and triplet cells with real transition energy, are studied. Particular emphasis is given to the tuning and optimisation of Negative Momentum Compaction (NMC) cells with imaginary transition energy. The optics of the high energy transfer line is also presented.

INTRODUCTION

Motivation

The replacement of the ageing CERN Proton Synchrotron (PS), which was constructed half a century ago, with a new ring (PS2), plays a key role in the overall upgrade strategy of the Large Hadron Collider (LHC) [1, 2]. The main purpose of the new ring is to ensure reliable operation over the coming decades and to enable the transmission of the ultimate beam needed for the LHC luminosity upgrade. The increased beam brightness and intensities should also enhance the opportunities of CERN's fixed target physics program.
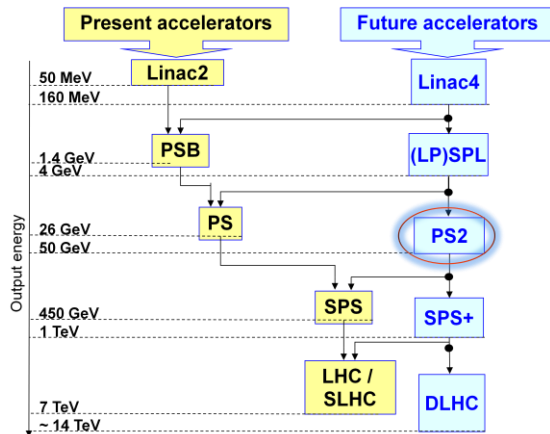

Figure 1: Output energy flowchart of the LHC injectors and collider at present and in the future, following a staged upgrade strategy [1].

Requirements

The PS2 should have the versatility of the existing PS, providing many different proton and ion beams, with various bunch patterns, for downstream accelerators or directly for physics experiments. In this respect, several injection and extraction systems must be implemented, including H⁻ charge exchange and fast ion injection,

conventional fast extraction for LHC, multi-turn extraction for SPS fixed target experiments and slow extraction for PS2 physics. Furthermore, the PS2 has to be integrated into the existing complex as part of a staged upgrade plan, presented schematically in Fig. 1 [1]. The upgrade scenario foresees the injection of proton beams into the PS2, directly from the Super-Conducting Proton Linac (SPL) [3, 4]. The low energy part of the SPL, called Linac4, will be constructed sooner, close to the PS complex, to provide 160 MeV H⁻ for the PS Booster [5]. The ion beams should be injected from the existing ion complex.
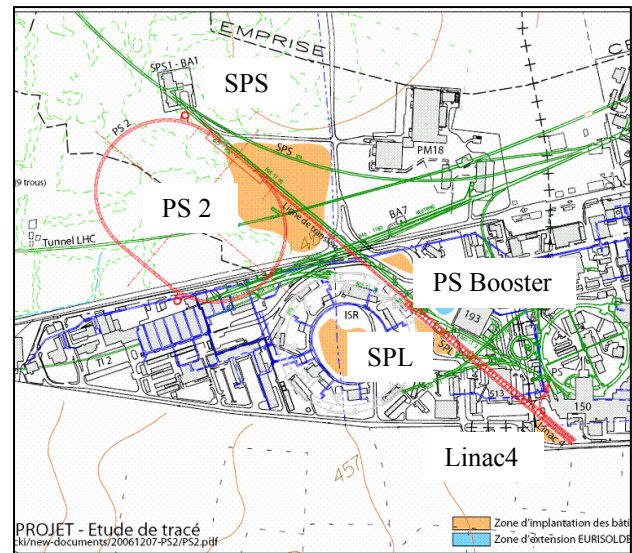

Figure 2: Layout of the PS2 integrated into the CERN accelerator complex.

A tentative layout of the PS2, integrated into the CERN accelerator complex, is shown in Fig. 2. The racetrack shape of the ring was dictated by the assumption that the SPL will be the proton injector for the PS2. In this respect, the injection and extraction systems are installed in one straight section [6]. The advantage of the racetrack shape is that the number of dispersion suppressors is reduced, which increases the bending filling factor and thereby the energy range that the synchrotron can reach. On the other hand, a racetrack shape with super-periodicity of only 2 will be quite susceptible to systematic linear and non-linear resonances, making the working point choice difficult. A supplementary constraint is imposed by the necessity to reduce H⁻ beam losses due to Lorentz stripping. Hence, the bending radius of the PS2 injection transfer line must be large and unnecessary bending must be avoided. Finally, the installation of the PS2 close to the SPS minimises the

length of the high-energy transfer line, but the optics constraints to be achieved become more difficult.

OPTICS DESIGN CONSTRAINTS

Some basic parameters that constrain the optics design of PS2 are displayed in Table 1, as compared to the ones of the present PS [7]. The kinetic energy at the PS2 extraction should be at least doubled in order to reduce the losses in the present SPS and limit the energy swing of a future machine with extraction energy of close to 1TeV. For reaching a 50 GeV kinetic energy with iron dominated magnets providing maximum bending field of 1.8T [8], the circumference of the ring should be at least doubled with respect to the 200π circumference of the PS. For optimum filling of the SPS for fixed target experiments with a 5-turn extraction from the PS2 and leaving some space for the SPS dump kicker, C_{PS2} should be less than one fifth of C_{SPS}, i.e. a bit longer than twice the circumference of the PS. Finally, the bunch patterns needed impose additional constraints in the circumference which was fixed to $C_{PS2} = \frac{15}{77}C_{SPS} = \frac{15}{7}C_{PS} = \frac{3000}{7}\pi$ [9].

Table 1: Basic beam parameters for PS2 as compared to the actual PS. Note that the PS is uses combined function magnets.

Basic beam parameters	PS	PS2
Injection kinetic energy [GeV]	1.4	4
Extraction kinetic energy [GeV]	13 / 25	50
Circumference [m]	200π	$3000\pi/7$
Transition energy [GeV]	6	~10/10i
Max. bending field [T]	1.2	1.8
Max. quadrupole gradient [T/m]	5	17
Max. beta functions [m]	23	60
Max. dispersion function [m]	3	6
Min. drift space for dipoles [m]	1	0.5
Min. drift space for quads [m]		0.8
Max. arc length [m]		510

The kinetic energy at injection is constrained by the maximum acceptable incoherent space charge tune-shift, which is scaled as $\Delta Q_{S.C.} \propto \frac{N_b}{\varepsilon_n \beta \gamma^2 B_f}$, i.e. proportional to the bunch population and inversely proportional to the normalised emittance ε_n, the bunching factor B_f and the square of the energy. In the PS, the space charge tune shift is around 0.2 for LHC-type beams at the 1.2ms injection plateau, a value considered as the maximum acceptable limit, for avoiding high beam losses due to resonance crossing. Considering that the number of protons per bunch for the LHC upgrade will be 4×10^{11} with respect to 1.7×10^{11} in the PS, the same normalised emittance and a bunching factor which is doubled due to the increase of the circumference of the ring, the injection

energy should be increased accordingly from 1.4 to around 4GeV.

The increase of both injection and ejection energies tends to slow down motion in longitudinal phase space and to increase longitudinal acceptances [10]. The choice of the main RF systems can be either a low-frequency large-bandwidth one, as in the actual PS, or a 40MHz system compatible with a pre-chopped beam coming from the SPL, but incompatible with the present scheme of heavy ion beam acceleration. The former system has the advantage of allowing different type of longitudinal manipulations, but it implies the increase of longitudinal acceptance and time needed for RF gymnastics, especially at high energy. The choice of the momentum compaction factor $\frac{1}{\gamma_{tr}^2} \approx \pm 0.01$ limits the aforementioned increase. Nevertheless, it constrains the transition energy to a real or imaginary value of around 10. The real transition energy is relatively straightforward to obtain with standard cells but necessitates the development of a low loss transition crossing scheme. The optics design of a Negative (or Flexible) Momentum Compaction (NMC) lattice leading to low imaginary transition energy is more challenging but has the obvious advantage of avoiding the problems of transition crossing and thus simplifying the whole acceleration process.
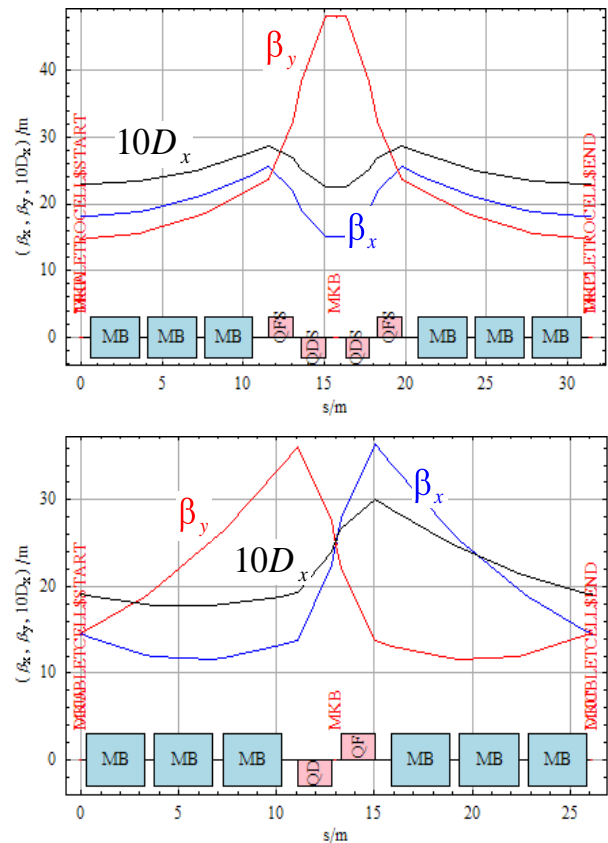

Figure 3: Optics functions for arc cells based on quadrupole doublets (bottom) and triplets (top).

The maximum quadrupole gradient is limited to below 17T/m giving a pole tip field of 1.3 T with 75mm pole radius [11], which leaves enough clearance for the

maximum beam sizes considered, taking into account the maximum optics functions quoted in Table 1.

The minimum drift lengths are set so as to leave enough space for placing other magnets such as orbit correctors, chromaticity sextupoles and instrumentation. Finally, the maximum arc length is set to around 510m, in order to leave enough space for the injection and extraction elements placed in the long straight sections.

LATTICE CONSIDERATIONS

Doublet and Triplet Lattices

Lattices based on quadrupole doublets and triplets (Fig. 3) allow longer drift sections for injection and extraction insertions. The triplet cells offer the additional feature of significantly reducing betatron functions in the long drift, which is an advantage for dipole apertures.
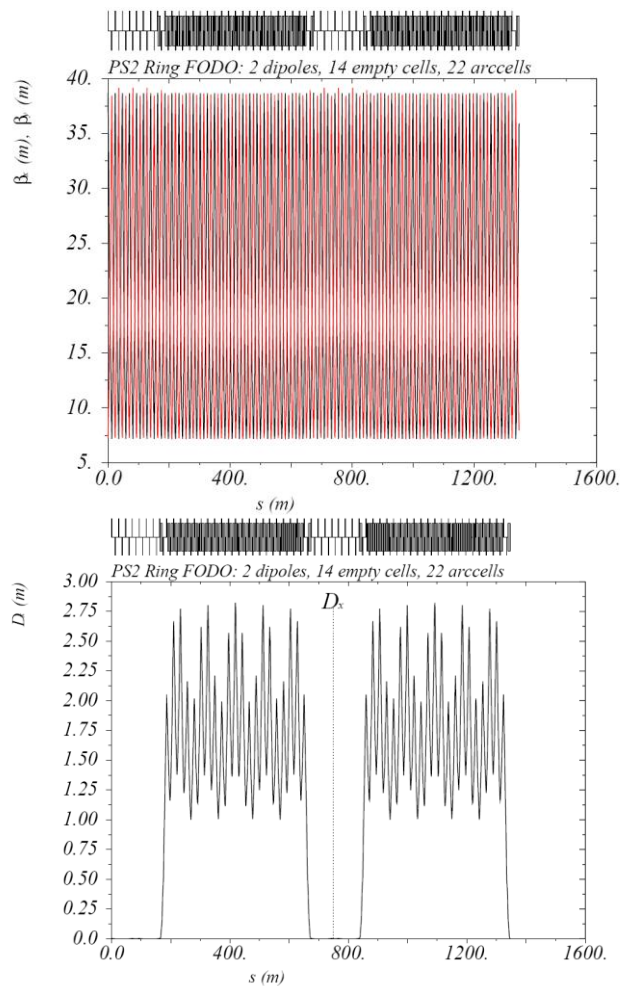

Figure 5: Lattice functions for the PS2 FODO lattice. Horizontal and vertical beta functions (top) and dispersion functions (bottom).

The main disadvantage of these lattice types is the strong focusing strength needed due to the small distance between adjacent quadrupoles, which exceeds the imposed gradient limit or requires longer quadrupoles, reducing the bending magnet filling factor. In consequence, there is insufficient space for the injection

and extraction systems for the imposed circumference and top energy.

FODO Lattice

The simplest lattice is based on plain FODO cells with two quadrupole families. With a phase advance of close to $\pi/2$ per cell, the dispersion can be suppressed naturally by a missing dipole scheme. The ring consists of 22 arc cells with four 3.8m-long dipoles per regular cell. The quadrupoles have all 1.5m length and their strength is within the imposed limit. The total length of the arc is around 510m. The optics functions' evolution along the whole ring is displayed in Fig. 5. Their maximum values are comfortably within the upper limits set in Table 1. The chosen phase advance per cell allows simple design of the transfer channels which can be located within the 7 cells of one of the long straight sections, as indicated in Fig. 6. This lattice achieves transition energies of around 11GeV for working points between 14.1 and 14.9 in both planes. The limited tunability of the lattice is its main drawback, as the two quadrupole families do not provide enough flexibility for exploring other working points. In this respect, an alternative FODO lattice with 10 quadrupole families has been also studied, with around 80° phase advance per cell, providing similar results with respect to optics functions, space constraints and transition energies reached.
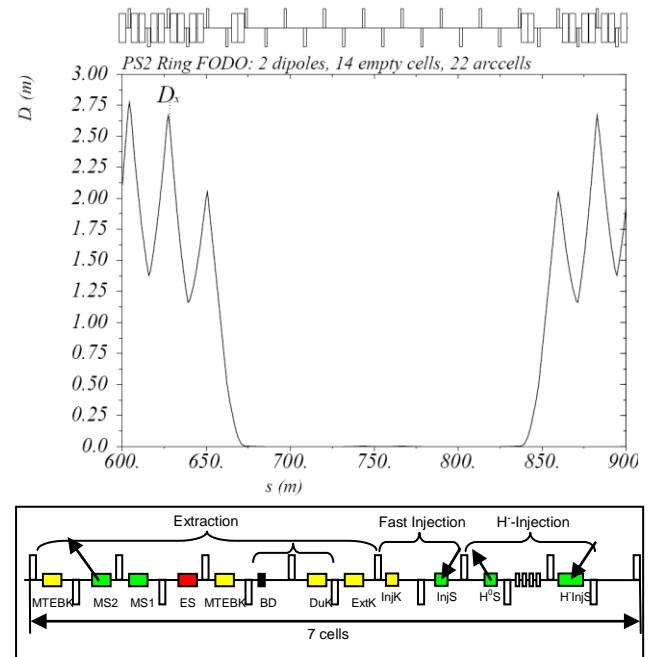

Figure 6: Dispersion suppression in the long straight section (top) and layout of all injection and extraction channels (bottom).

NMC Modules

NMC modules similar to the ones studied in detail in the 90's [13,14] and built recently for the high energy synchrotron of the J-PARC project [15] have been investigated [16]. The first module studied for PS2 starts

from an almost regular FODO focusing structure shown in the upper part of Fig. 7, with one special cell without bends surrounded by two filled cells. The phase advance per cell is matched to the desired value. The plot corresponds to phase advance of 90°, bringing the dispersion at the beginning and at the end of the module to zero. The drifts in the central cell are then reduced and the quadrupole strengths of the centre are rematched to the desired average phase advance per cell to obtain the lattice in the lower plot. Following this method, the low imaginary transition energy of 10i can be obtained. The main disadvantage is that the vertical beta function exceeds by far the imposed limit (it gets close to 80m).
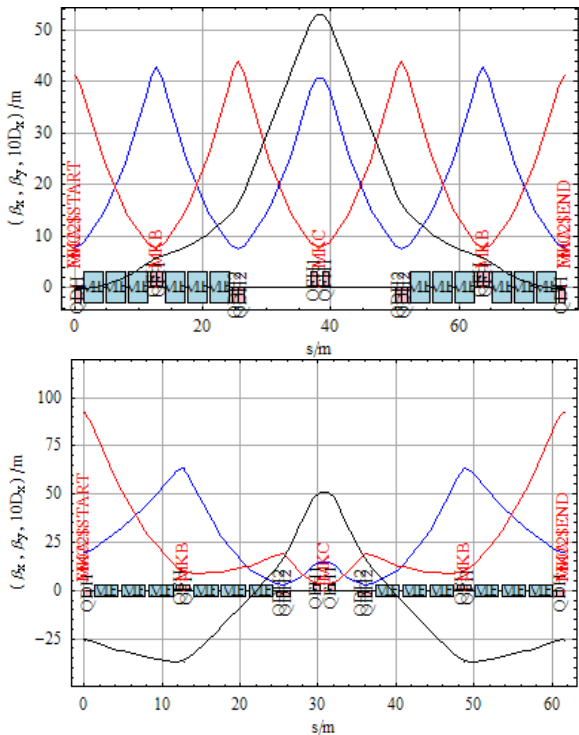

Figure 7: Horizontal (blue), vertical (red) beta functions and dispersion (black), for NMC module starting from regular FODO cells (top) and reducing central drifts (bottom).

Another NMC module is shown in Fig. 8. The bending filling factor is improved by increasing the number of FODO cells from 3 to 4, i.e. adding a half FODO cell with bends from either side of the previous module. In that way, the phase advance per cell can be lowered and, at the same time, a very low imaginary gamma transition can be obtained.

The functioning of the module is depicted in the upper plot showing the trace of the normalised dispersion vector $(\frac{D_x}{\sqrt{\beta_x}}, D_x'\sqrt{\beta_x} + D_x\frac{\alpha_x}{\sqrt{\beta_x}})$, for one module. The effect of the cells filled with bends is indicated by a single jump in the dispersion invariant and in thin lens approximation (the correct evolution of the dispersion vector is plotted as a dashed line). The radius of the induced dispersion beating can be adjusted with the overall phase advance inside the module. Large radii and thus negative

contributions to the momentum compaction can be obtained with a phase advance slightly smaller than 2π.

By choosing appropriate phase advances tuned by 4 families of quadrupoles, the module can give relatively low imaginary transition energy. In the example presented on Fig. 9, for horizontal and vertical phase advances of 280° and 320°, respectively, imaginary transition energy of 8.2i can be obtained. The main drawback of this module is its length of around 96m which leaves very little space for the long straight section.
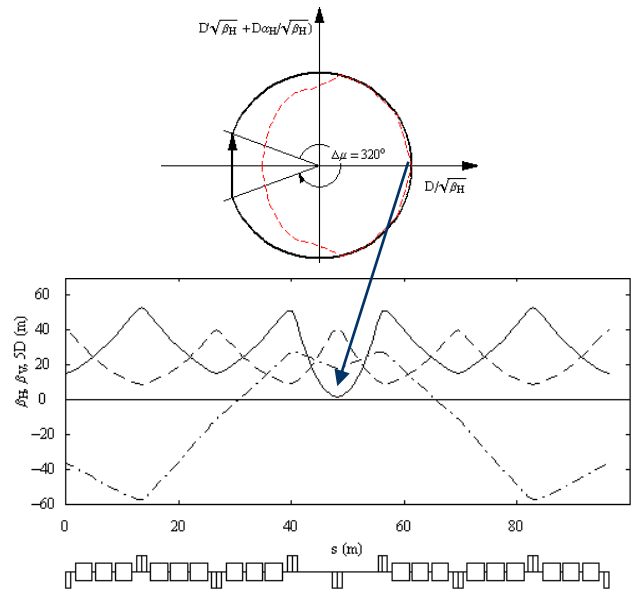

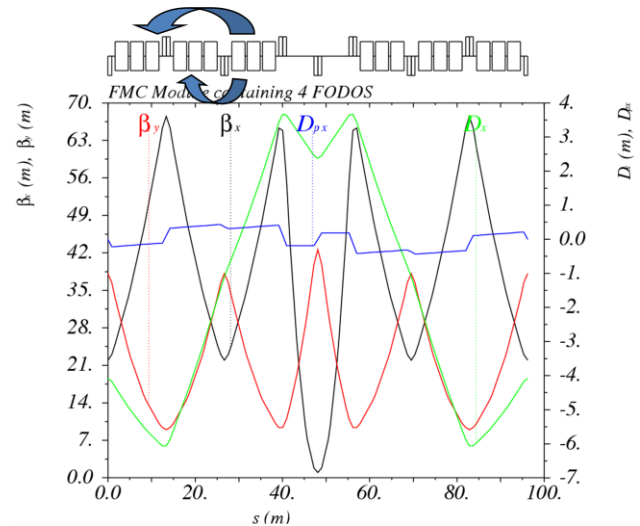Figure 8: NMC module with increased filling factor.

Figure 9: NMC module with increased filling factor and low imaginary transition energy.

A modified module can be obtained by moving the bending magnets of the most internal half cell towards the exterior parts of the module. The momentum compaction factor defined as $\alpha_c = \frac{1}{C}\oint\frac{D(s)}{\rho(s)}ds$ will become even smaller, as the bending magnets are pushed to areas where the dispersion is negative. At the same time, the space between the bend-free cells can be further squeezed, thus diminishing drastically the size of the

whole module. An example of the NMC described above is given on the top of Fig. 10, consisting of one FODO cell with four bending magnets per half cell and a quadrupole doublet. All quadrupoles in half of the module are powered individually setting the total number to 5 families. For phase advances of 320º, in both planes, imaginary transition energy of around 6i can be achieved. For driving the momentum compaction factor to such low negative values in a limited space while keeping the beta functions below 60m, the dispersion has big excursions from -8 to 6m. The arc can be built with 5 of this modules plus a dispersion supressors of around the same length giving an estimated total length of 560m, which still does not leave enough space for the long straight section elements.
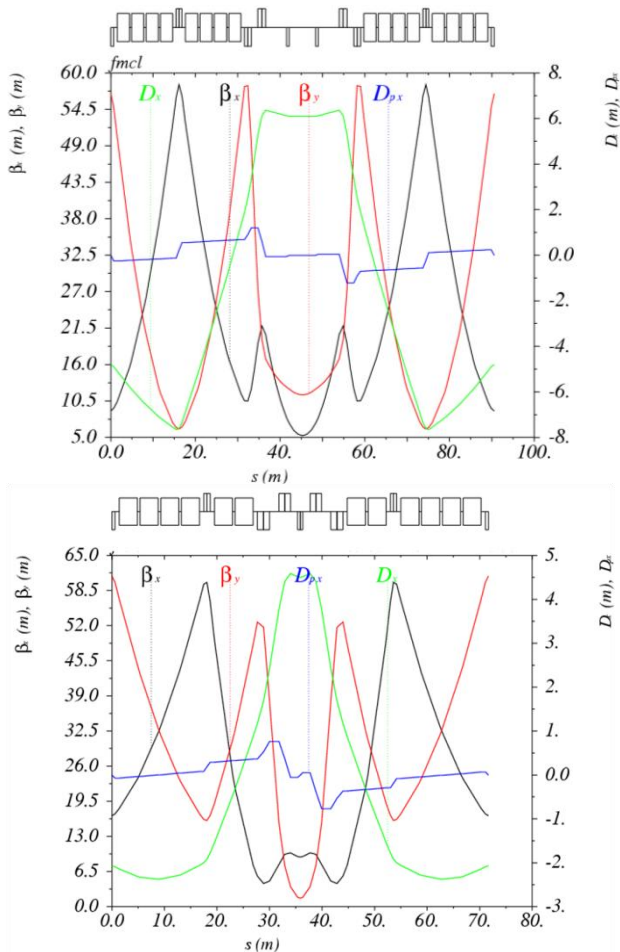

Figure 10: Optics functions of short NMC modules with high filling factor and low imaginary transition energy, leaving reasonable space for the long straight sections.

In order to shorten this module, one could first cut down the number of dipoles in the second FODO half cell and than reduce the space in the center of the module, having one instead of two central quadrupoles (bottom of Fig.10). This assymetric FODO cell module satisfies all the criteria from the point of view of optics functions maxima. For phase advances of around 270º and 260º degrees in the horizontal and vertical plane, it provides imaginary transition energy of 10i. The clear advantage of

this module is its length, which is around 70m. With 7 modules of this type plus dispersion suppressors having equal length in total, the arc length can be below the required 510m.
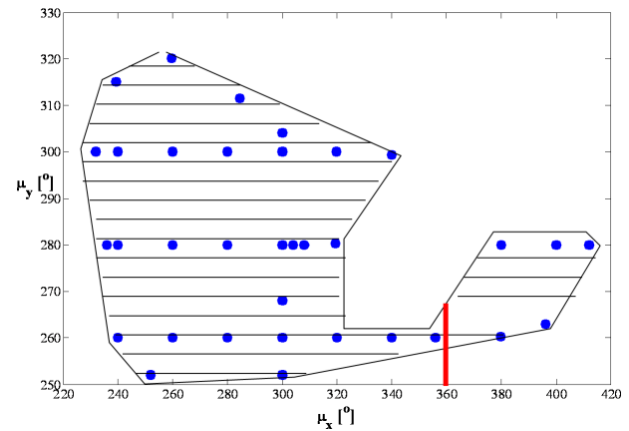

Figure 11: Phase advances achieved from the short high-filling-factor NMC module.

In Fig.11, the possible phase advances achieved by this module are shown. The blue dots are a few matched cases, for which all the imposed optics, gradient and length constraints are satisfied, but the tuning of the module is pretty flexible and it covers all the shaded area, i.e. phase advances of 240º to 420º in the horizontal plane and 250º to 320º in the vertical plane. The red dash marks the 360º horizontal phase advance which cannot be reached, as the optics become unstable.
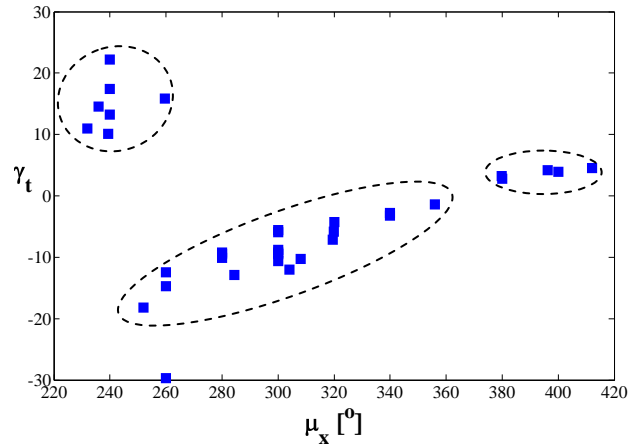

Figure 12: Phase advances achieved from the short high-filling-factor NMC module. The negative part of the vertical axis corresponds to imaginary transition energies.

All the matched phase advances do not necessarily correspond to imaginary transition energies. In Fig. 12, the horizontal phase advance is plotted versus the transition energy. Imaginary transition energies correspond to the negative part of the vertical axis for plotting simplicity. The diagram can be roughly divided in three parts. The upper left part, for which the horizontal phase advance is particularly low, corresponds to real transition energies. The middle part corresponds to imaginary values going from 20i down to 2i for horizontal

phase advances very close to 2π. Above 360°, solutions with very low real transition energies can be achieved.

Apart from the dependence of the transition energy on the phase advance, there is also an almost linear dependence of the momentum compaction factor (inverse square of the transition energy) to the extremum value of the dispersion as shown in Fig. 13, where the transition energy is plotted against the maximum and minimum values of the dispersion function. For low imaginary or real transition energy the excursion of the dispersion function is getting to very high values and certainly above the imposed 6m limit. The dispersion function is getting much more relaxed for high transition energies.
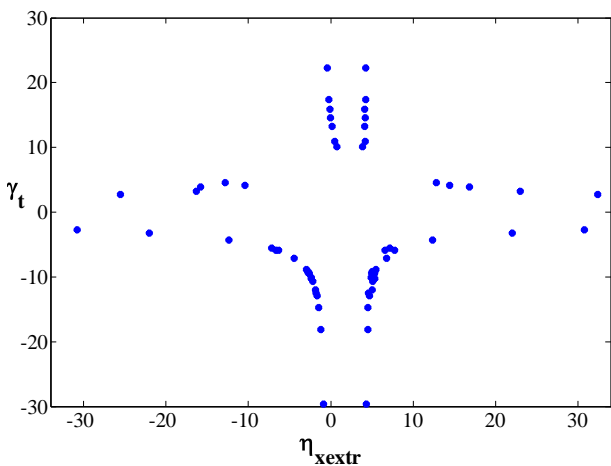

Figure 13: Transition energy versus dispersion minimum and maximum values. The negative part of the vertical axis corresponds to imaginary transition energies.

Finally, the dependence of the chromaticity on transition is plotted in Fig. 14, where the blue dots correspond to horizontal and red to the vertical plane. For lower transition energies, the horizontal chromaticity tends to become higher. The vertical chromaticity is certainly independent of the transition energy. It is mostly restricted by the matching conditions to achieve the vertical phase advance of the different options.

The challenge of this type of modules is to construct a dispersion suppressor that would also match the optics' functions in the long straights. The structure along with the lattice functions of a possible dispersion supressor are depicted in Fig. 15. The first half module is exactly a copy of the arc NMC module. The second part of the module where the dispersion is matched to zero while keeping the beta variation under control uses 4 independent quadrupole families and it is necessary to add a fifth dipole in the last half FODO cell. With this dispersion supressor the whole arc has the required length of 510m and the long straight section can be matched without difficulty to form the rest of the ring. The main drawback is the high horizontal beta function of around 70m, that has to be reduced by relaxing some space contraints or by accepting a slighlty higher imaginary transition energy.
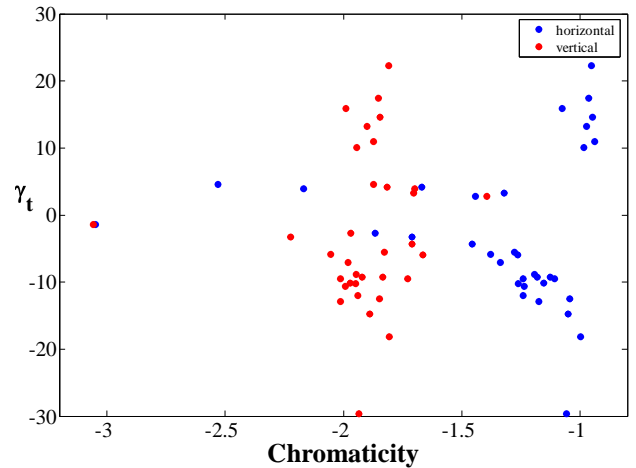

Figure 14: Transition energy versus horizontal (blue) and vertical (red) chromaticity. The negative part of the vertical axis corresponds to imaginary transition energies.
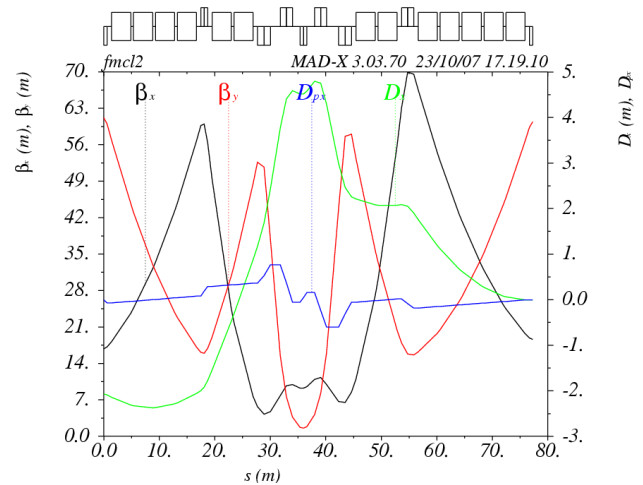

Figure 15: Optics functions evolution along the NMC module dispersion suppressor.

HIGH ENERGY TRANSFER LINE

The high energy transfer line has to match the PS2 optics into the SPS with the tight geometry and length requirements of the proposed layout (see Fig. 16). It should also accommodate a stripping foil for Pb ions, which necessitates a low beta insertion. The use of normal conducting magnets with adequate fields and gradients is a reasonable choice. The transfer line may necessitate an emittance exchange scheme as in the present PS to SPS transfer line and a branch to serve the future experimental areas of the PS2. Vertical bending magnets are not necessary as the PS2 will be constructed at the same level as the SPS.

Studies of possible solutions were made using two main achromat bends in the middle of a 360m-long line. This design provides the adequate separation required between the PS2 machine and the existing transfer tunnels. A matching section with a low beta insertion for the stripping foil location was designed near the SPS. The emittance exchange scheme remains challenging due to the space constraints (additional cells have to be

added). The design of the injection and experimental area transfer lines are in progress.

SUMMARY AND PERSPECTIVES

Optics considerations to define a suitable lattice for the proposed PS2 machine were presented. The plain FODO lattice is a good candidate and a straightforward choice. A transition crossing scheme should be implemented to complete the linear lattice design.
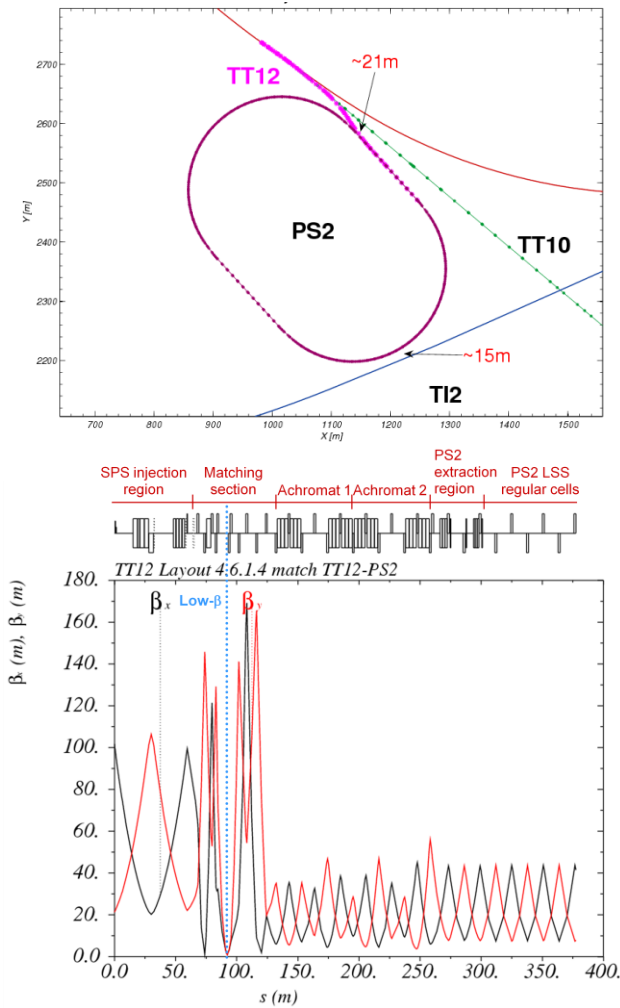

Figure 16: Layout of the PS2 to SPS transfer line (top) and beta function evolution for a proposed optics design solution (bottom).

Alternative negative momentum compaction lattices were investigated. In particular, a short high-filling-factor module satisfies all optics constraints. An optics parameter scan demonstrated the difficulty to keep the low imaginary transition energy of 10i, while keeping the optics functions (especially dispersion) below the imposed limit of 6m. A dispersion suppressor for arc cells based on this module was designed giving a total arc length which is short enough to accommodate the long straight section injection and extraction insertions.

The study will be completed including chromaticity correction, orbit, gradient, coupling and non-linear multipole error analysis and dynamic aperture simulations. The detailed comparison between the two options (real or imaginary transition energy) should be based on the performance of the lattices against beam losses, which implies a careful design of a collimation system and non-linear dynamics considerations including the impact of space charge and other collective effects.

ACKNOWLEDGEMENTS

REFERENCES

[1] R. Garoby, these proceedings.

[2] M. Benedikt, R. Garoby, F. Ruggiero, R. Ostojic, W. Scandale, E. Shaposhnikova, J. Wenninger, "Preliminary Accelerator Plans for Maximising the integrated LHC Luminosity", CERN-AB-2006-018-(PAF).

[3] R. Garoby, M. Benedikt, A. Fabich, F. Gerigk, "Comparison of Options for the Injector of PS2", CERN-AB-2007-014 (PAF).

[4] F. Gerigk, these proceedings.

[5] M. Vretenar, these proceedings.

[6] M. Barnes, M. Benedikt, J. Borburgh, T. Fowler, B. Goddard, "PS2 Beam Transfer Systems: Conceptual Design Considerations", CERN internal AB-Note-2007-001.

[7] M. Benedikt, "General Design Aspects for the PS2", Proceedings of LUMI'06 Valencia, CERN-2007-002.

[8] T. Zickler, "Design study of normal-conducting magnets for the CERN PS2", CERN internal AT-MEL Technical Note, edms:855337.

[9] R. Garoby, "RF Constraints on the Size of PS2", CERN internal AB-Note-2007-020.

[10] S. Hancock, "Gamma at Transition of the proposed PS2 Machine", CERN internal AB-Note-2006-39.

[11] M. Benedikt, "Preliminary requirements for the design of PS2 magnets", CERN internal AB-Note-2007-29.

[13] S. Y. Lee, K. Y. Ng, D. Trbojevic, "Minimising dispersion in flexible–momentum-compaction lattices", Physical Review E, Vol.48, No 4, p. 3040-3048.

[14] U. Wienands, et al., "The High-γ_t lattice for the SSC low energy booster", Proceeding of HEACC'92, Hamburg.

[15] "Accelerator Technical Design Report for JPARC", KEK Report 2002-13.

[16] W. Bartmann, M. Benedikt, C. Carli, B. Goddard, S. Hancock, J.-M. Jowett, Y. Papaphilippou, "Optics considerations for the PS2", Proceedings of 2007 Particle Accelerator Conference, Albuquerque, NM, USA, 25 - 29 Jun 2007, p.739-741.